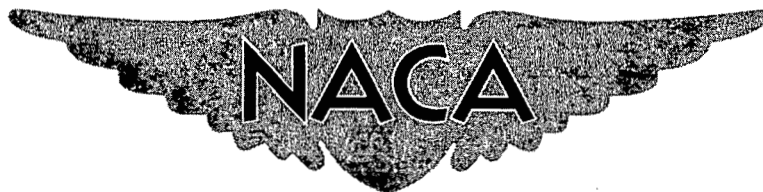


C-7

Copy  
RM L55A18

~~CONFIDENTIAL~~

NACA RM L55A18



# RESEARCH MEMORANDUM

EXPERIMENTAL FLUTTER INVESTIGATION OF A THIN UNSWEPT  
WING AT TRANSONIC SPEEDS

By George L. Pratt

Langley Aeronautical Laboratory  
Langley Field, Va.

CLASSIFICATION CHANGED

UNCLASSIFIED

Authority of *RA + RN-112* Date *2-8-57*  
*NB 3-12-57*

CLASSIFIED DOCUMENT

This material contains information affecting the National Defense of the United States within the meaning of the espionage laws, Title 18, U.S.C., Secs. 793 and 794, the transmission or revelation of which in any manner to an unauthorized person is prohibited by law.

## NATIONAL ADVISORY COMMITTEE FOR AERONAUTICS

WASHINGTON

April 4, 1955

~~CONFIDENTIAL~~

## NATIONAL ADVISORY COMMITTEE FOR AERONAUTICS

## RESEARCH MEMORANDUM

EXPERIMENTAL FLUTTER INVESTIGATION OF A THIN UNSWEPT  
WING AT TRANSONIC SPEEDS

By George L. Pratt

## SUMMARY

Zero-lift experimental flutter data have been obtained in the Mach number range from 0.75 to 1.25 on a 1.5-percent-thick, untapered, unswept, solid steel wing having hexagonal airfoil sections and wing length-to-chord ratios of 1.61 and 1.73. The wing was tested as a cantilever with and without a half-body-of-revolution fuselage. The test data indicated that reflected fuselage bow waves had an effect on the flutter results at Mach numbers from approximately 1.05 to 1.20; hence, the discussion and conclusions are confined mainly to the data obtained with the fuselage removed.

The results of the test of the wing at a length-to-chord ratio of 1.61 and with the fuselage removed indicated that calculated flutter speeds based on two-dimensional, incompressible-flow aerodynamic coefficients were approximately 15 to 20 percent less than the experimental values at Mach numbers from 0.875 to 1.175; this difference increased at the higher test Mach numbers. An aspect-ratio correction resulted in calculated flutter speeds which were 10 to 15 percent greater than the experimental values at Mach numbers from 0.875 to 1.175; this difference decreased at the higher test Mach numbers. Except at the higher Mach numbers, the analytic solutions satisfactorily predicted the variation of flutter speed with mass ratio, but the calculated flutter speeds based on two-dimensional aerodynamic coefficients were approximately 15 to 20 percent less than the experimental values.

## INTRODUCTION

Only a limited amount of research has been done experimentally and analytically to determine the effect of various design parameters on the flutter characteristics of wings at transonic speeds. (Some of the more recent experimental research is contained in refs. 1 to 4.) The nature of the airloads on wings at transonic speeds complicates flutter analysis

CONFIDENTIAL

and increases the need for experimental flutter research. Such research provides the flutter data necessary to check various analytic methods of flutter prediction and provides data for empirical studies. An investigation has been inaugurated in the Langley 9- by 12-inch blowdown tunnel to provide experimental data indicating the effect of various wing geometric, elastic, and mass parameters on the flutter characteristics of wings at transonic speeds.

The present paper contains the results of the part of this investigation concerning the zero-lift experimental flutter data obtained in the Mach number range from 0.75 to 1.25 on a 1.5-percent-thick, unswept, untapered, solid steel wing having hexagonal airfoil sections. Tests were made with the wing cantilever-mounted from the tunnel floor at a wing length-to-chord ratio of 1.61. For some of the tests, the wing was cantilever-mounted from a half-body-of-revolution fuselage on the floor of the tunnel at aspect ratios of 3.75 and 4.00 which correspond to exposed-wing length-to-chord ratios of 1.61 and 1.73, respectively.

The experimental flutter speeds, reduced flutter speeds, and flutter frequencies have been normalized by using flutter values calculated by the strip-analysis procedure of reference 5 with aerodynamic coefficients for incompressible flow. In addition, three-dimensional aerodynamic effects are taken into account for the case of the wing without the fuselage by applying an aspect-ratio correction determined by the method of reference 6.

The present data are the initial flutter data obtained in the test facility, and because of the large ratio of wing plan-form area to test-section cross-sectional area, some comment on the reliability of the flutter data obtained is warranted. Although some effect of the reflection of the model fuselage bow wave from the tunnel walls at certain Mach numbers is indicated in the present paper, it is believed that the test facility is satisfactory for flutter-testing, particularly when the effects of the fuselage bow wave have been eliminated. This belief is based on the satisfactory results obtained in this facility in static tests of models of similar size and on the results of reference 1 which indicate that satisfactory flutter data can be obtained in transonic slotted wind tunnels.

#### NOTATION

- A aspect ratio including body intercept
- a nondimensional elastic-axis position measured from mid-chord, positive rearward, semichords

b	wing semichord, in. or ft (as required by dimensional considerations)
c	wing chord, 2b, in.
$f_{h_1}$	first bending natural frequency, cps
$f_{h_2}$	second bending natural frequency, cps
$f_\alpha$	uncoupled first torsion frequency about elastic axis, cps
g	structural damping coefficient
$\xi_h$	structural damping coefficient for bending mode
$\xi_\alpha$	structural damping coefficient for torsion mode
$I_\alpha$	wing mass moment of inertia about elastic axis per unit length, lb-sec <sup>2</sup>
$I_{xx}$	wing section area moment of inertia, in. <sup>4</sup>
l	length of exposed wing measured perpendicular to wing root, in.
M	Mach number
m	mass of wing per unit length, lb-sec <sup>2</sup> /sq in.
q	dynamic pressure at flutter, $\frac{1}{2}\rho V_e^2$ , lb/sq ft
$r_\alpha$	nondimensional radius of gyration of wing about elastic axis, $\sqrt{I_\alpha/mb^2}$ , fraction of semichord
t	wing thickness, in.
V	stream velocity at flutter, ft/sec
$x_\alpha$	nondimensional wing section center-of-gravity location measured from elastic axis, positive rearward of elastic axis, percent of semichord

~~CONFIDENTIAL~~

$\rho$	air density at flutter, slugs/cu ft or lb-sec <sup>2</sup> /in. <sup>4</sup> (as required by dimensional considerations)
$\mu$	mass ratio at flutter, $m/\pi\rho b^2$
$\omega$	flutter frequency, radians/sec
$\omega_h$	first bending natural frequency, radians/sec
$\omega_\alpha$	uncoupled first torsion frequency about elastic axis, radians/sec

## Subscripts:

e	experimental value at flutter
R	based on strip-analysis method of reference 5 with two-dimensional aerodynamic coefficients
A	based on aspect-ratio correction of reference 6

## MODEL, APPARATUS, AND TESTS

## Model

The wing was untapered, unswept, and of solid steel construction with a hexagonal airfoil section. The chord was 2 inches and the thickness-to-chord ratio was 0.015. Various other wing geometric and mass parameters are listed in table 1. Figure 1 shows a sketch of the model arrangement with the fuselage installed. The fuselage was a half-body of revolution mounted on the floor of the tunnel with a 1/4-inch shim to extend the model beyond the tunnel-floor boundary layer. The wing was clamped rigidly at the wing-fuselage juncture and the aspect ratio could be changed by merely loosening the clamp and sliding the untapered wing through the fuselage. A sketch of the fuselage is presented in figure 1. With the fuselage installed, the wing was tested at aspect ratios of 3.75 and 4.00. These aspect ratios correspond to exposed-wing length-to-chord ratios  $l/c$  of 1.61 and 1.73, respectively. The wing was tested without the fuselage by cantilever-mounting the wing from the tunnel floor at  $l/c = 1.61$ .

The measured natural bending and torsion frequencies for the wings at the two aspect ratios and without the fuselage are presented in

table II. Inasmuch as the elastic axis and center of gravity coincide on the wing, these frequencies correspond to the uncoupled frequencies.

### Wind Tunnel

The wind tunnel used in this investigation was the Langley 9- by 12-inch blowdown tunnel incorporating a transonic test section. The transonic test section is 7 inches high and 10 inches wide and is slotted longitudinally along the top and side walls. Without a model installed in the test section, tunnel surveys indicate that the maximum deviation of the Mach number from the average test-section Mach number over the length of the test section is  $\pm 0.005$  at  $M = 0.75$  and increases to  $\pm 0.020$  at  $M = 1.25$ . Semispan models are cantilever-mounted from the floor of the test section.

The tunnel stagnation pressure can be varied from atmospheric pressure to approximately 31 lb/sq in. abs by means of a throttling valve located upstream of the test section. The Mach number is controlled by means of a cylindrical plunger located in the closed-wall part of the tunnel downstream of the test section. The plunger can be extended into the airstream and chokes the tunnel at the desired Mach number. This arrangement of throttling valve and Mach number control plunger permits the Mach number and stagnation pressure to be changed independently.

An air dryer and heater is installed upstream of the test section to eliminate any condensation effects.

In order to stop the flutter before the wing fluttered to destruction, a quick-acting butterfly valve located upstream of the test section could be closed. The butterfly valve stopped the flow of air in the tunnel in less than 1 second.

### Apparatus and Instrumentation

Strain gages were installed on the surface of the wing near the root to indicate the bending and torsion frequencies and to establish the occurrence of flutter. (Visual observation of the wing was restricted and the bending and torsion modes during flutter were difficult to discern.) The signal from the strain gages was amplified and fed into a recording oscillograph to obtain the time histories of the flutter motion.

The tunnel test conditions were obtained by photographically recording the tunnel stagnation and static pressures (indicated on a manometer board) and the tunnel stagnation temperature simultaneously with each oscillograph record.

## Test Procedure

The wing flutter points were obtained by approaching the flutter condition by two procedures: (1) setting the tunnel stagnation pressure at a desired value and changing the Mach number in small increments until the model fluttered and (2) setting the Mach number control plunger in a desired position and varying the test-section density by increasing the tunnel stagnation pressure in small increments until flutter was obtained. In many instances it was found convenient to vary alternately both the Mach number and stagnation pressure during the course of obtaining a flutter point.

During a test, the vibrations of the wing caused by the turbulence of the flow in the tunnel were believed to be of sufficient amplitude so that external excitation of the wing to initiate flutter was not considered necessary.

## RESULTS AND DISCUSSION

### Presentation of Data

The flutter data obtained with the wing are presented in the form of plots of several experimental flutter parameters ( $q$ ,  $\omega_e/\omega_\alpha$ ,  $V_e/b\omega_e$ ) plotted against the Mach number at which the data were obtained (fig. 2). For the purpose of providing a basis for comparing the results of the present investigation with results for other wings, an attempt has been made to account for the effects of such flutter parameters as  $\mu$ ,  $\omega_h/\omega_\alpha$ ,  $a$ ,  $x_\alpha$ , and  $r_\alpha$  by normalizing the data by using calculated reference flutter speeds and frequencies. These normalized data are presented in figure 3 as a function of Mach number. In order to provide a direct comparison indicating the effect of the fuselage on the flutter characteristics of the wing, the values of  $V_e/V_R$  obtained for the wing with and without the fuselage at  $l/c = 1.61$  are presented in figure 4. Sections of the oscillograph-record bending and torsion traces from which the flutter frequencies were determined are shown in figure 5 for several Mach numbers. In figures 6 and 7 the effect of the mass ratio  $\mu$  on the wing flutter characteristics is indicated. (The quantity  $\omega_h/\omega_\alpha$  was constant for any particular length-chord ratio and  $a$ ,  $x_\alpha$ , and  $r_\alpha$  were constant for the test wing throughout the present investigation.) Table III presents the experimental and analytical results obtained with the fuselage removed and the wing cantilever-mounted from the tunnel floor at  $l/c = 1.61$ .

### Calculated Flutter Speeds and Frequencies

Two analytic methods have been utilized to calculate the reference flutter speeds and frequencies used to normalize the flutter data. The first method of analysis is based on two-dimensional, incompressible-flow, oscillating-airfoil aerodynamic coefficients. The solution was obtained by applying the strip-analysis method of reference 5 for a wing of zero sweep oscillating in two degrees of freedom and by employing the uncoupled first bending and uncoupled first torsion mode shapes of a uniform cantilever beam. The calculated reference flutter speeds and frequencies of this analysis are denoted by the subscript R throughout the paper.

The second analytic solution differs from the above solution only in that it employs the aspect-ratio corrections of reference 6. The reference flutter speeds and frequencies determined by this method of solution are denoted by the subscript A.

In these two methods, the flutter determinant was solved at various values of reduced flutter speed  $V/b\omega$  and mass ratio  $\mu$  for the damping coefficient  $g$ . The paired value of  $V/b\omega$  from a plot of  $V/b\omega$  against  $g$  for a specific value of  $\mu$  at which  $g_h = g_\alpha = g = 0$  was taken to be the reference flutter point.

### Effect of Fuselage

In the initial phase of the investigation, the wing was cantilever-mounted from a half-body of revolution as indicated in figure 1. The flutter data obtained through the test Mach number range for aspect ratios of 4.00 ( $l/c = 1.73$ , figs. 2(a) and 3(a)) and 3.75 ( $l/c = 1.61$ , figs. 2(b) and 3(b)) with this arrangement indicate a sharp deviation from the trend of the flutter points with Mach number in the proximity of  $M = 1.05$  as shown by the large scatter in the data. A reason for this scatter in the data appeared to be that the reflection of the fuselage bow shock wave from the tunnel walls back to the model might be of sufficient strength to affect the flutter characteristics of the wing even at the lower supersonic Mach numbers.

In order to eliminate any effects of the fuselage bow wave, the fuselage was removed and the wing was cantilever-mounted from the floor of the tunnel at the same exposed-wing length-to-chord ratio ( $l/c = 1.61$ ) as the  $A = 3.75$  wing-fuselage configuration. The tunnel-floor boundary layer at the root of the model was considered to have relatively little effect on the flutter characteristics of the model.

With the fuselage removed, the deviation in the trend of the data with Mach number was eliminated near  $M = 1.05$ . In addition, there was

a variation in the magnitude of the data from approximately  $M = 1.05$  to  $M = 1.20$ . Simple shock-reflection theory indicates that, in this Mach number range, shock waves from the fuselage bow might be expected to reflect back onto the wing from the tunnel walls. Figure 4 shows the maximum variation in the flutter-speed ratio resulting from fuselage effects to be approximately 0.08 at  $M = 1.17$ . Inasmuch as the fuselage-bow-wave reflections appear to have an effect on the flutter characteristics of the wing, the remainder of the discussion is confined to the data obtained with the fuselage removed and with the wing cantilever-mounted from the tunnel floor at an exposed-wing length-to-chord ratio  $l/c$  of 1.61.

#### Variation of Wing Flutter Characteristics With Mach Number

An examination of the experimental flutter data for the wing at  $l/c = 1.61$  (fig. 2(c)) indicates that less dynamic pressure  $q$  is required to flutter the model as sonic velocity is approached but that increasingly higher dynamic pressures are required before flutter will occur at Mach numbers greater than  $M = 1.175$ . Figure 2(c) also shows the variation of the ratio of the flutter frequency to the first natural torsion frequency  $\omega_e/\omega_t$  and the variation of the reduced flutter speed  $V_e/b\omega_e$  with Mach number for the test wing and indicates a considerable effect of Mach number on the wing flutter frequencies. Figure 5 presents sections of the oscillograph-record bending and torsion traces obtained at various Mach numbers from which the flutter frequencies were determined.

#### Results of Analytic Solutions

The variations with Mach number shown by the normalized flutter data (fig. 3(c)) indicate that there is a considerable effect of Mach number on the flutter characteristics of the wing. Some variation might be expected, particularly through the transonic speed range where the flow over the wing is in the transition range from subsonic to supersonic speed, because the attendant changes in the magnitudes and phases of the air forces and in the location of the aerodynamic center with these flow changes are not accounted for by the two-dimensional incompressible-flow aerodynamic coefficients.

In general, the calculated flutter speeds based on two-dimensional, incompressible-flow aerodynamic coefficients  $V_R$  were approximately 15 to 20 percent less than the experimental values from  $M = 0.875$  to  $M = 1.175$  (fig. 3(c)). The aspect-ratio correction resulted in calculated flutter speeds  $V_A$  which were 10 to 15 percent greater than the experimental values from  $M = 0.875$  to  $M = 1.175$  (fig. 3(c)). At the

Mach numbers above  $M = 1.175$  the flutter-speed ratios  $V_e/V_R$  and  $V_e/V_A$  increased with an increase in Mach number.

The analytic solutions utilized did not accurately predict the flutter frequencies as indicated by the values of flutter-frequency ratio  $\omega_e/\omega_R$  and  $\omega_e/\omega_A$  (fig. 3(c)).

#### Variation of Wing Flutter Characteristics With Mass Ratio

In figures 6 and 7, various experimental and normalized flutter parameters are plotted against the square root of the mass ratio at flutter. Since the effect of Mach number cannot be disregarded in a comparison such as this, the data have been separated into groups corresponding to various parts of the Mach number range by using approximately the inflection points of the  $V_e/V_R$  plots of figure 3(c) to separate the various groupings ( $M < 0.975$ ,  $0.975 < M < 1.050$ ,  $1.050 < M < 1.175$ , and  $M > 1.175$ ).

The data indicate that, in general, the variation of  $V_e/b\omega_\alpha$  with  $\sqrt{\mu}$  was essentially the same as predicted by the two analytic solutions except at the highest Mach numbers, but there was a difference in magnitude (approximately 15 to 20 percent) between the experimental and calculated values based on the two-dimensional aerodynamic coefficients (fig. 6). The parameters  $V_e/b\omega_e$  and  $\omega_e/\omega_\alpha$  differed both in magnitude and trend with  $\sqrt{\mu}$  from those predicted by the analytic solutions.

#### CONCLUSIONS

The results of the flutter tests of a thin unswept wing at transonic speeds indicated:

1. For the wing cantilever-mounted without the fuselage at a length-to-chord ratio of 1.61, calculated flutter speeds based on incompressible-flow, two-dimensional aerodynamic coefficients were approximately 15 to 20 percent less than the experimental values at Mach numbers from 0.875 to 1.175. This difference increased at the higher Mach numbers at which flutter data were obtained.

2. An aspect-ratio correction resulted in calculated flutter speeds which were 10 to 15 percent greater than the experimental values at Mach numbers from 0.875 to 1.175. This difference decreased at the higher Mach numbers at which flutter data were obtained.

3. Except at the higher Mach numbers, the analytic solutions satisfactorily predicted the variation of flutter speed with mass ratio but the calculated flutter speeds based on the two-dimensional aerodynamic coefficients were approximately 15 to 20 percent less than the experimental values.

4. There was some effect of reflections of the fuselage bow wave from the tunnel walls between Mach numbers of 1.05 to 1.20. The maximum variation in flutter-speed ratio was 0.08 at a Mach number of 1.170 between the fuselage-on and fuselage-off conditions.

Langley Aeronautical Laboratory,  
National Advisory Committee for Aeronautics,  
Langley Field, Va., January 13, 1955.

## REFERENCES

1. Bursnall, William J.: Initial Flutter Tests in the Langley Transonic Blowdown Tunnel and Comparison With Free-Flight Flutter Results. NACA RM L52K14, 1953.
2. Jones, George W., Jr., and DuBose, Hugh C.: Investigation of Wing Flutter at Transonic Speeds for Six Systematically Varied Wing Plan Forms. NACA RM L53G10a, 1953.
3. D'Ewart, B. B., and Ryken, J. M.: Cantilever Wing Flutter Model Tests at Low and Transonic Speeds. Rep. No. 02-941-022A, Bell Aircraft Corp., 1953. (Also available as USAF Tech. Rep. No. 53-47, Wright Air Dev. Center, U. S. Air Force, 1953.)
4. Herrera, Raymond, and Barnes, Robert H.: An Experimental Investigation of the Flutter of Several Wings of Varying Aspect Ratio, Density, and Thickness Ratio at Mach Numbers From 0.60 to 1.10. NACA RM A54A29, 1954.
5. Barmby, J. G., Cunningham, H. J., and Garrick, I. E.: Study of Effects of Sweep on the Flutter of Cantilever Wings. NACA Rep. 1014, 1951. (Supersedes NACA TN 2121.)
6. Reissner, Eric, and Stevens, John E.: Effect of Finite Span on the Airlord Distributions for Oscillating Wings. II - Methods of Calculation and Examples of Application. NACA TN 1195, 1947.

TABLE I.- GEOMETRIC, MASS, AND INERTIA  
CHARACTERISTICS OF THE WING

$t$ , in. . . . .	0.030
$c$ , in. . . . .	1.998
$a$ . . . . .	0
$x_{\alpha}$ . . . . .	0
$m$ , lb-sec <sup>2</sup> /sq in. . . . .	$37.44 \times 10^{-6}$
$\frac{m}{2}$ or $\rho\mu$ , lb-sec <sup>2</sup> /in. <sup>4</sup> . . . . .	11.94
$\pi b^2 I_{xx}$ , in. <sup>4</sup> . . . . .	$3.52 \times 10^{-6}$
$I_{\alpha}$ , lb-sec <sup>2</sup> . . . . .	$9.30 \times 10^{-6}$
$r_{\alpha}^2$ . . . . .	0.248

TABLE II.- WING NATURAL FREQUENCIES

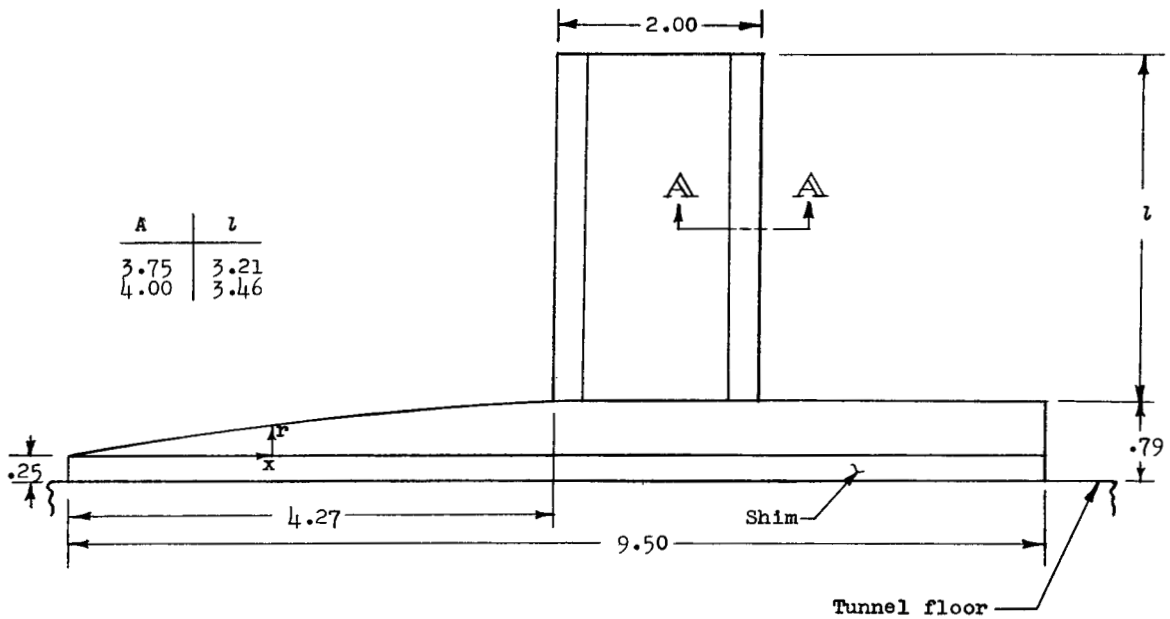
$l/c$	A	$f_{h_1}$	$f_{h_2}$	$f_{\alpha}$	$\frac{\omega_{h_1}}{\omega_{\alpha}}$	Fuselage
1.61	3.75	89	---	352	0.253	On
1.61	----	89	---	352	.253	Off
1.73	4.00	74	460	326	.227	On

TABLE III.- EXPERIMENTAL AND ANALYTICAL RESULTS FOR WING

CANTILEVER-MOUNTED FROM TUNNEL FLOOR

$$[z/c = 1.61]$$

M	$\frac{q}{lb/sq\ ft}$	$\mu$	$\frac{V_e}{ft/sec}$	$f_e,$ cps	$\frac{\omega_e}{\omega_\alpha}$	$\frac{V_e}{b\omega_e}$	$\frac{\omega_e}{\omega_R}$	$\frac{V_e}{V_R}$	$\frac{V_e}{b\omega_\alpha}$
0.874	1,419	79.8	946	153	0.433	11.80	0.887	1.203	5.11
.887	1,411	83.5	964	148	.419	12.45	.862	1.202	5.22
.907	1,353	89.9	980	150	.425	12.47	.880	1.178	5.30
.911	1,384	90.7	995	143	.406	13.29	.841	1.194	5.40
.918	1,346	92.7	992	139	.394	13.64	.818	1.177	5.37
.928	1,323	94.0	991	139	.394	13.62	.819	1.168	5.37
.940	1,293	100.7	1,014	136	.385	14.23	.805	1.154	5.48
.944	1,281	100.2	1,006	131	.371	14.67	.775	1.149	5.44
.950	1,276	104.1	1,024	131	.371	14.94	.778	1.148	5.54
.960	1,254	106.7	1,028	129	.366	15.22	.769	1.140	5.57
.966	1,243	114.0	1,061	126	.358	16.08	.756	1.140	5.76
.974	1,235	112.9	1,049	120	.340	16.69	.718	1.131	5.68
.983	1,229	113.9	1,052	114	.323	17.61	.682	1.128	5.69
.984	1,257	111.3	1,051	114	.323	17.61	.681	1.141	5.69
.988	1,335	107.4	1,064	117	.331	17.36	.696	1.172	5.75
.990	1,250	113.7	1,059	115	.326	17.59	.689	1.139	5.73
.990	1,263	111.5	1,054	114	.323	17.67	.681	1.144	5.71
.993	1,289	111.0	1,063	116	.329	17.49	.694	1.156	5.75
.997	1,351	106.8	1,067	115	.329	17.72	.691	1.192	5.83
1.000	1,327	107.9	1,063	119	.337	17.06	.709	1.171	5.75
1.011	1,438	101.4	1,073	122	.346	16.79	.724	1.219	5.81
1.012	1,401	106.1	1,083	120	.341	17.25	.716	1.207	5.88
1.012	1,439	101.4	1,073	121	.343	16.94	.718	1.220	5.81
1.012	1,399	104.8	1,076	120	.340	17.13	.713	1.202	5.82
1.022	1,427	105.1	1,087	122	.346	17.02	.726	1.215	5.89
1.029	1,447	104.4	1,092	121	.343	17.23	.719	1.222	5.91
1.035	1,460	104.8	1,099	123	.349	17.06	.732	1.229	5.95
1.036	1,491	102.1	1,096	122	.346	17.17	.724	1.242	5.94
1.036	1,468	104.4	1,100	122	.346	17.21	.726	1.232	5.96
1.042	1,457	107.8	1,113	123	.349	17.28	.734	1.229	6.03
1.045	1,478	104.5	1,104	---	---	---	---	---	---
1.050	1,466	108.9	1,123	121	.344	17.72	.724	1.234	6.10
1.064	1,467	109.7	1,127	119	.337	18.09	.710	1.231	6.10
1.064	1,451	110.6	1,125	117	.332	18.37	.700	1.229	6.10
1.069	1,471	112.0	1,140	120	.341	18.14	.720	1.238	6.19
1.073	1,425	113.8	1,132	113	.320	19.12	.676	1.213	6.12
1.074	1,422	117.8	1,150	116	.330	18.93	.699	1.218	6.25
1.082	1,409	120.2	1,156	116	.330	19.04	.700	1.214	6.28
1.088	1,445	116.4	1,152	117	.331	18.79	.701	1.220	6.22
1.098	1,440	120.5	1,170	119	.338	18.77	.718	1.225	6.34
1.112	1,455	118.2	1,165	119	.337	18.70	.714	1.227	6.30
1.114	1,475	120.3	1,183	121	.344	18.68	.730	1.241	6.43
1.123	1,434	121.8	1,174	118	.334	19.00	.709	1.217	6.35
1.145	1,453	124.0	1,192	120	.340	18.96	.723	1.226	6.45
1.161	1,445	126.8	1,203	123	.348	18.68	.742	1.224	6.50
1.166	1,412	130.0	1,202	122	.346	18.81	.739	1.213	6.51
1.170	1,405	140.1	1,246	120	.341	19.84	.732	1.213	6.77
1.177	1,443	130.4	1,219	124	.352	18.77	.752	1.227	6.61
1.182	1,448	130.8	1,223	123	.348	18.98	.743	1.224	6.61
1.190	1,518	126.1	1,229	127	.360	18.49	.767	1.257	6.66
1.193	1,540	123.7	1,226	127	.360	18.43	.766	1.264	6.64
1.202	1,584	122.2	1,236	130	.368	18.16	.782	1.281	6.68
1.211	1,555	127.5	1,251	130	.369	18.37	.787	1.273	6.78
1.218	1,630	119.6	1,241	130	.368	18.22	.781	1.300	6.71
1.222	1,650	120.3	1,252	133	.377	17.97	.800	1.308	6.78
1.224	1,700	116.8	1,252	137	.388	17.46	.821	1.326	6.77
1.246	1,800	113.5	1,266	142	.402	17.03	.849	1.360	6.85



Fuselage Ordinates	
x	r
0	0
0.54	.09
1.08	.18
1.62	.26
2.17	.33
2.71	.39
3.25	.44
3.79	.49
4.33	.52
4.87	.54
5.41	.54
9.50	.54

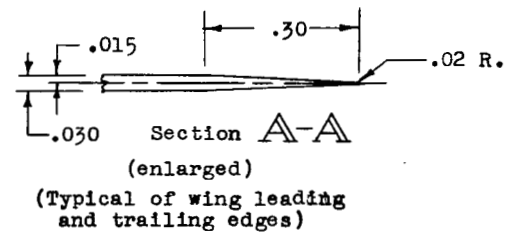
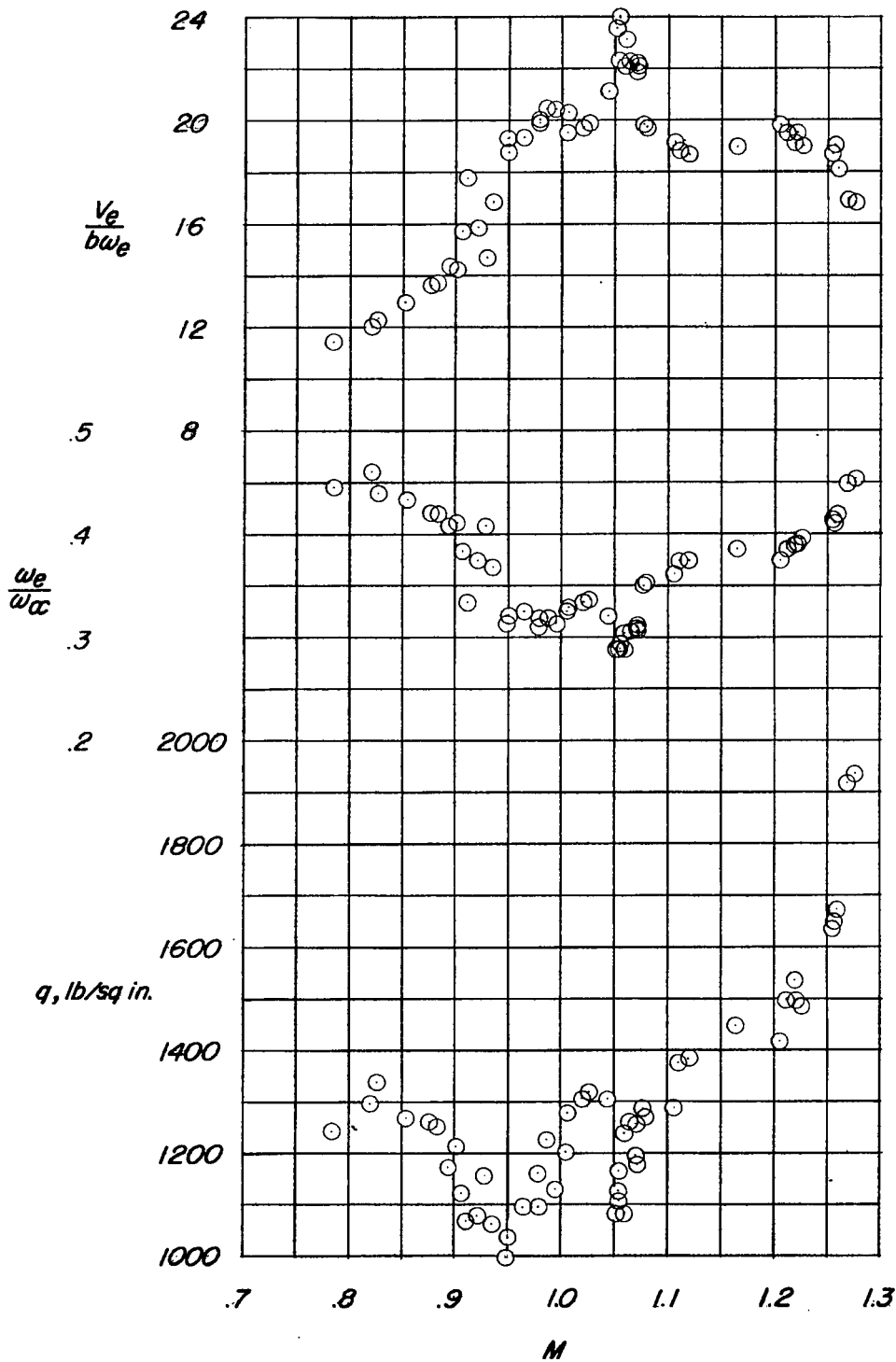
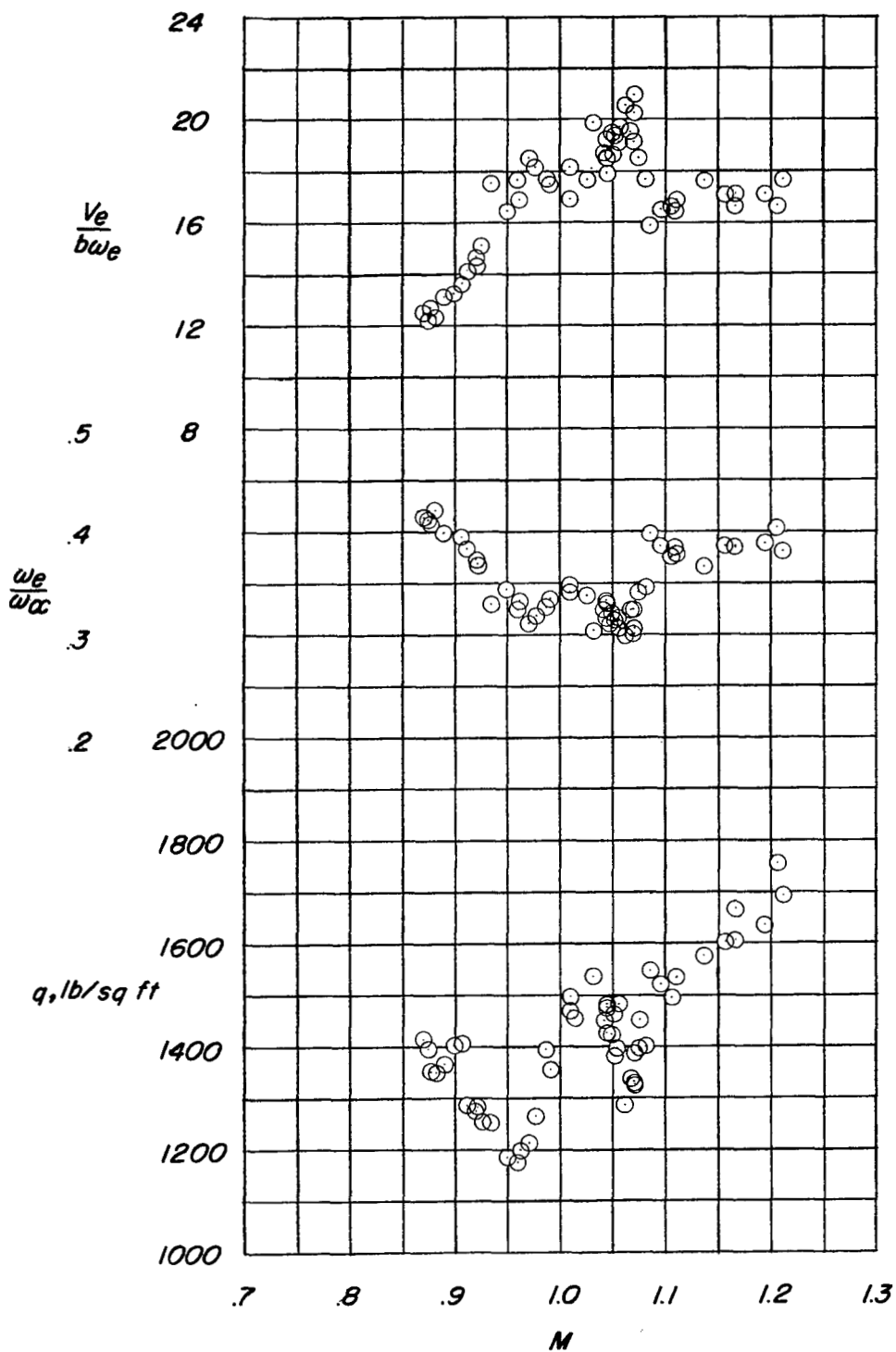


Figure 1.- Sketch of wing-fuselage arrangement. Dimensions in inches.



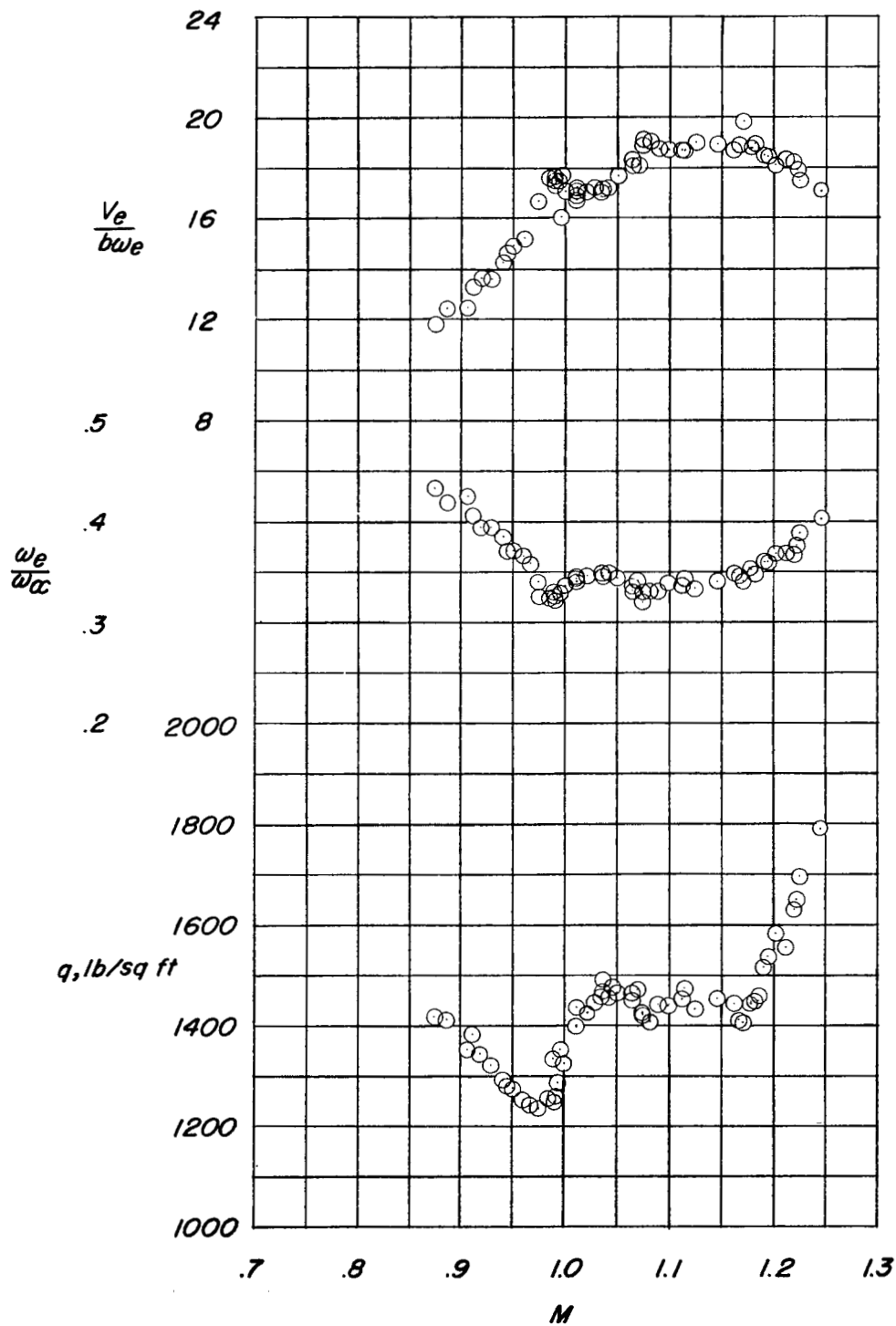
(a)  $A = 4.00$ ;  $l/c = 1.73$ ; fuselage installed.

Figure 2.- Experimental flutter characteristics plotted against Mach number.



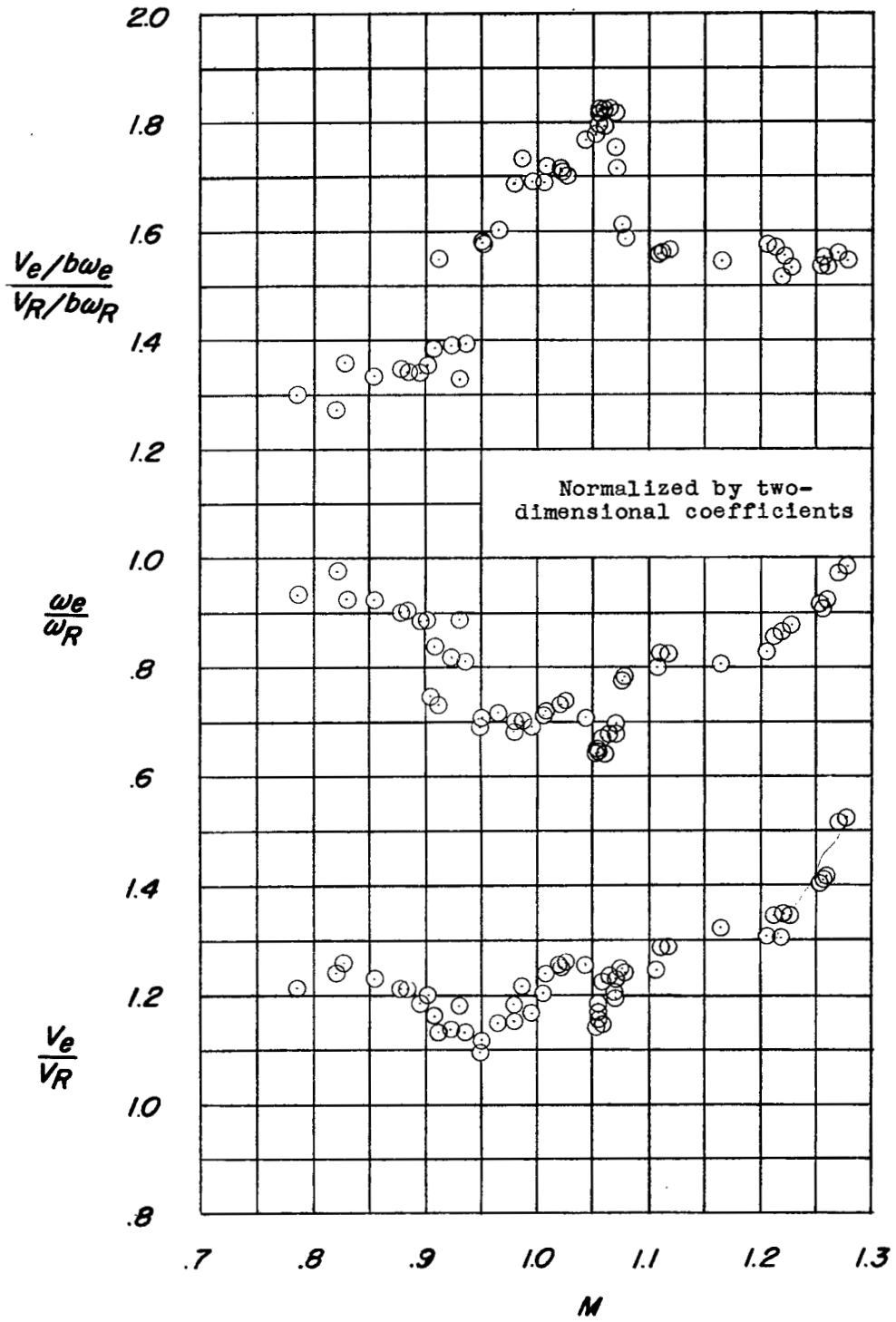
(b)  $A = 3.75$ ;  $l/c = 1.61$ ; fuselage installed.

Figure 2.- Continued.



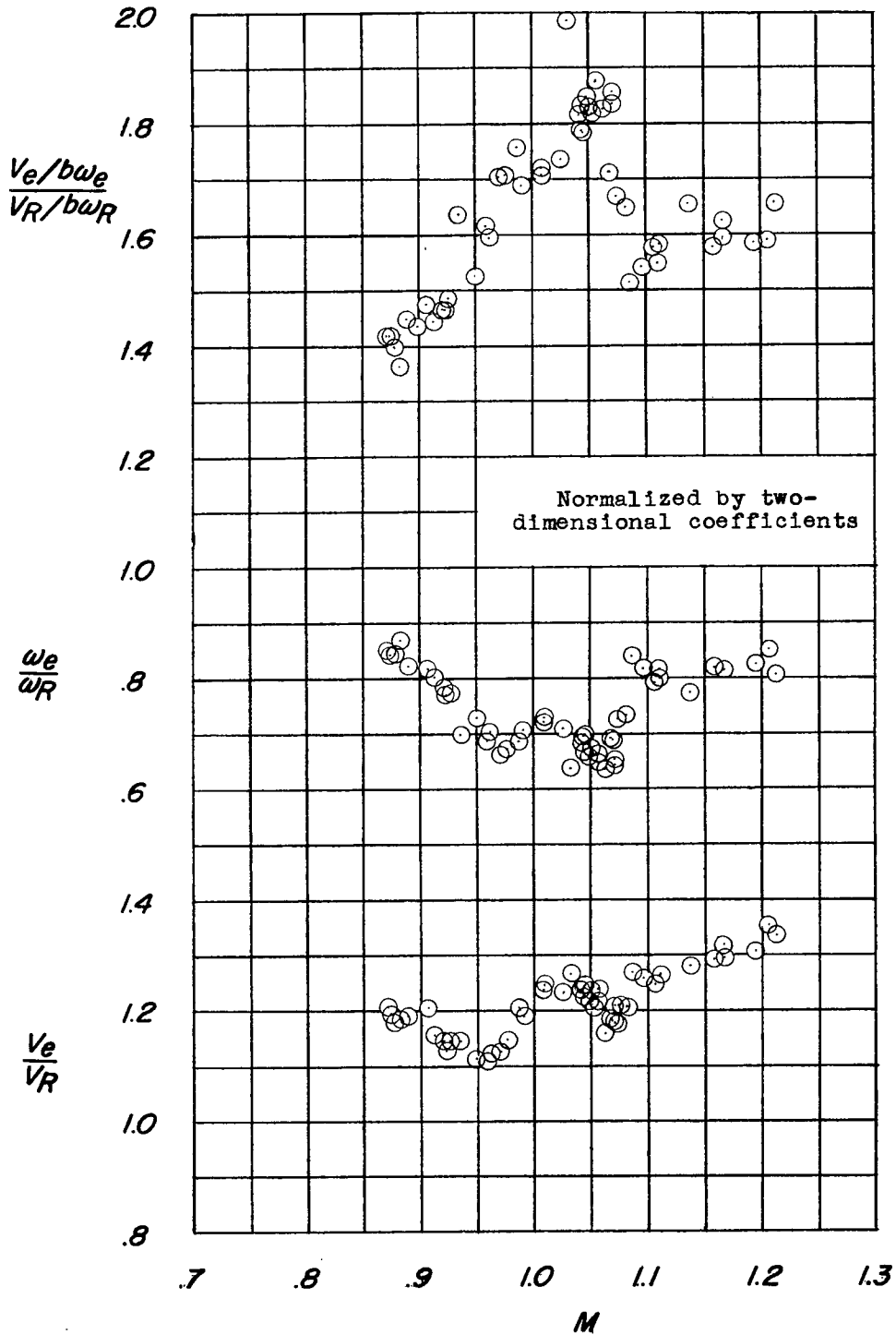
(c)  $l/c = 1.61$ ; no fuselage.

Figure 2.- Concluded.



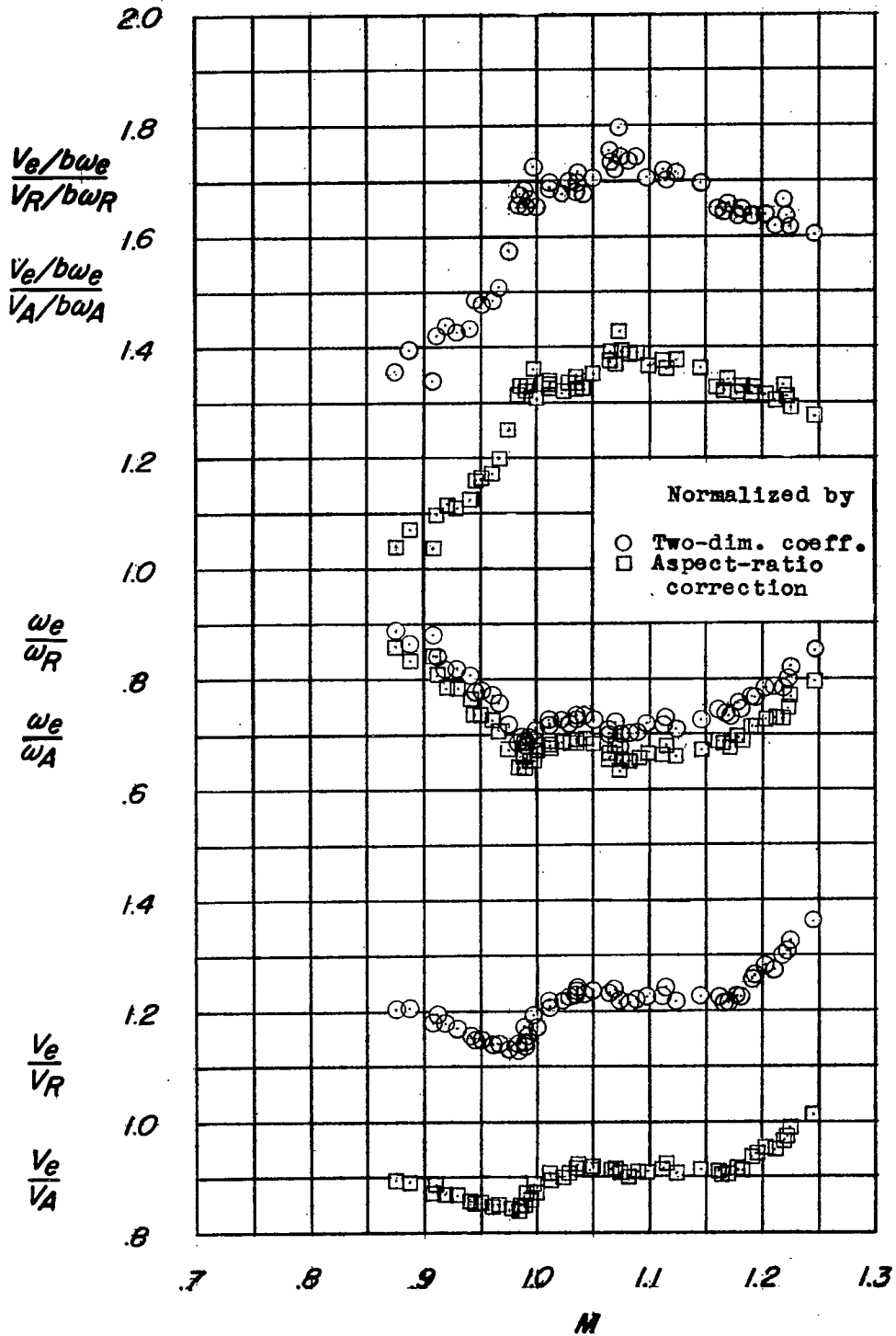
(a)  $A = 4.00$ ;  $l/c = 1.73$ ; fuselage installed.

Figure 3.- Normalized flutter characteristics plotted against Mach number.



(b)  $A = 3.75$ ;  $l/c = 1.61$ ; fuselage installed.

Figure 3.- Continued.



(c)  $l/c = 1.61$ ; no fuselage.

Figure 3.- Concluded.

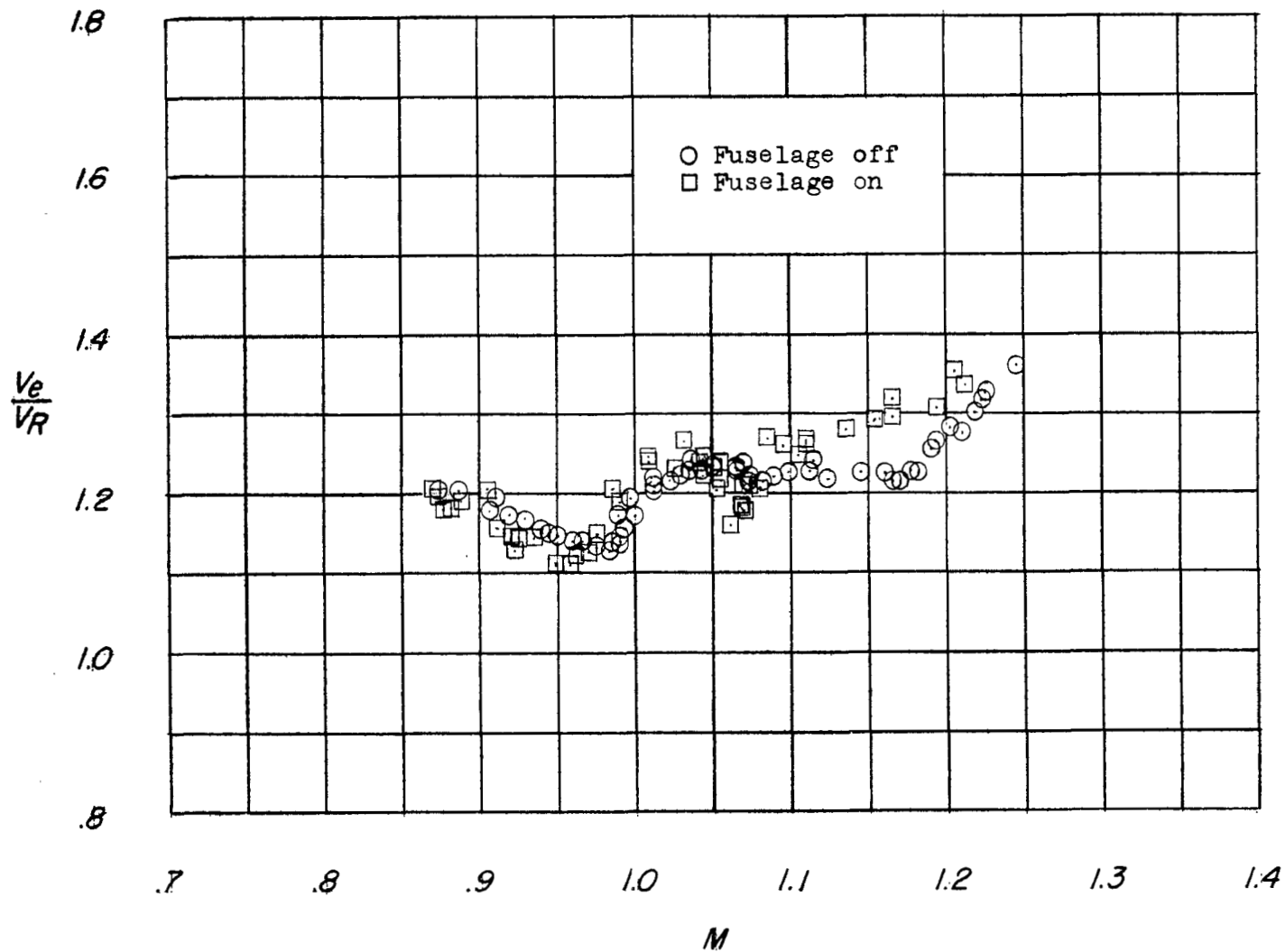


Figure 4.- Comparison of flutter speed ratios for wing with and without fuselage installed.  $l/c = 1.61$ ;  $A = 3.75$ .

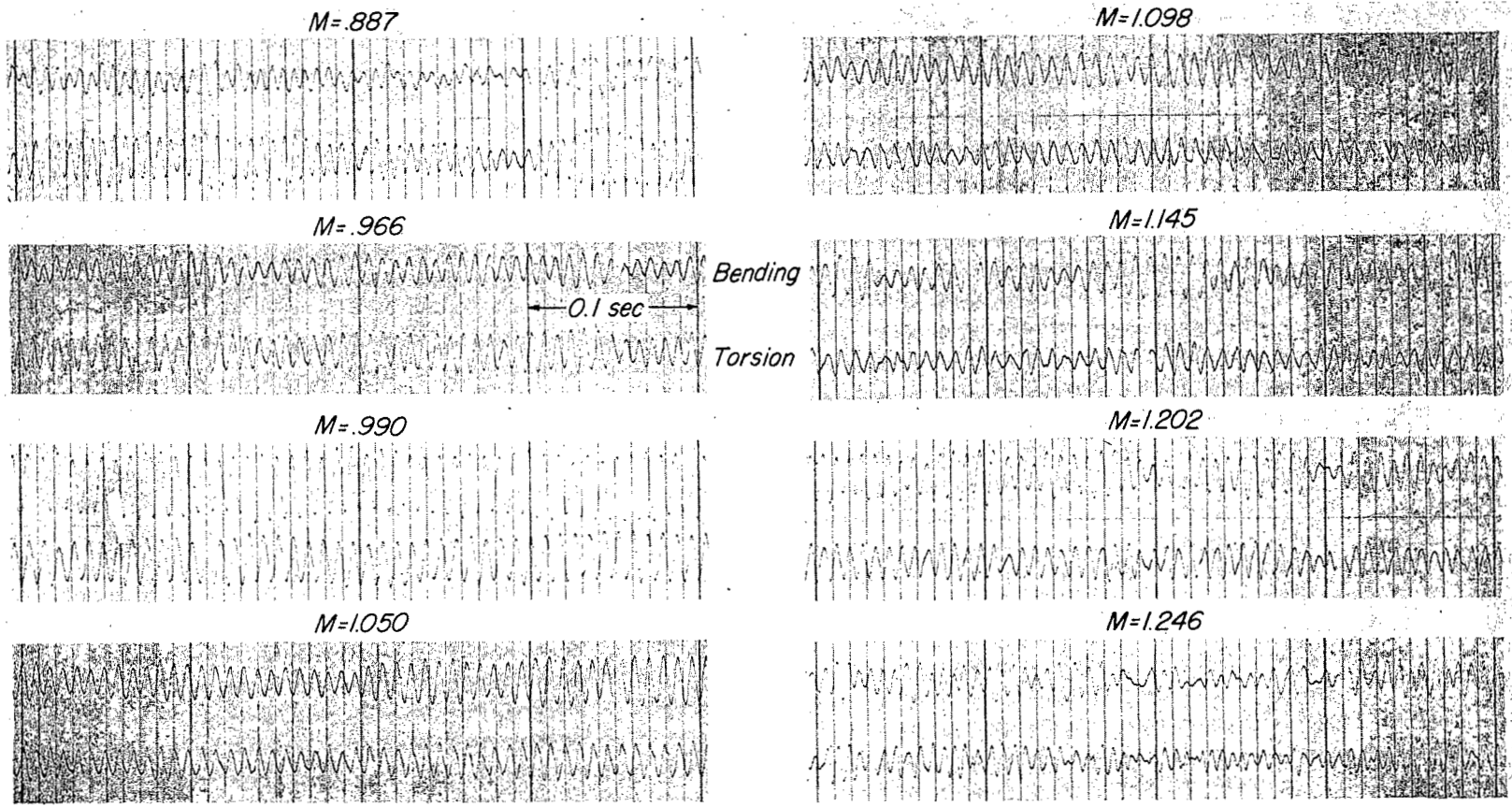


Figure 5.- Sections of oscillograph-record bending and torsion traces at several Mach numbers.  $l/c = 1.61$ ; no fuselage.

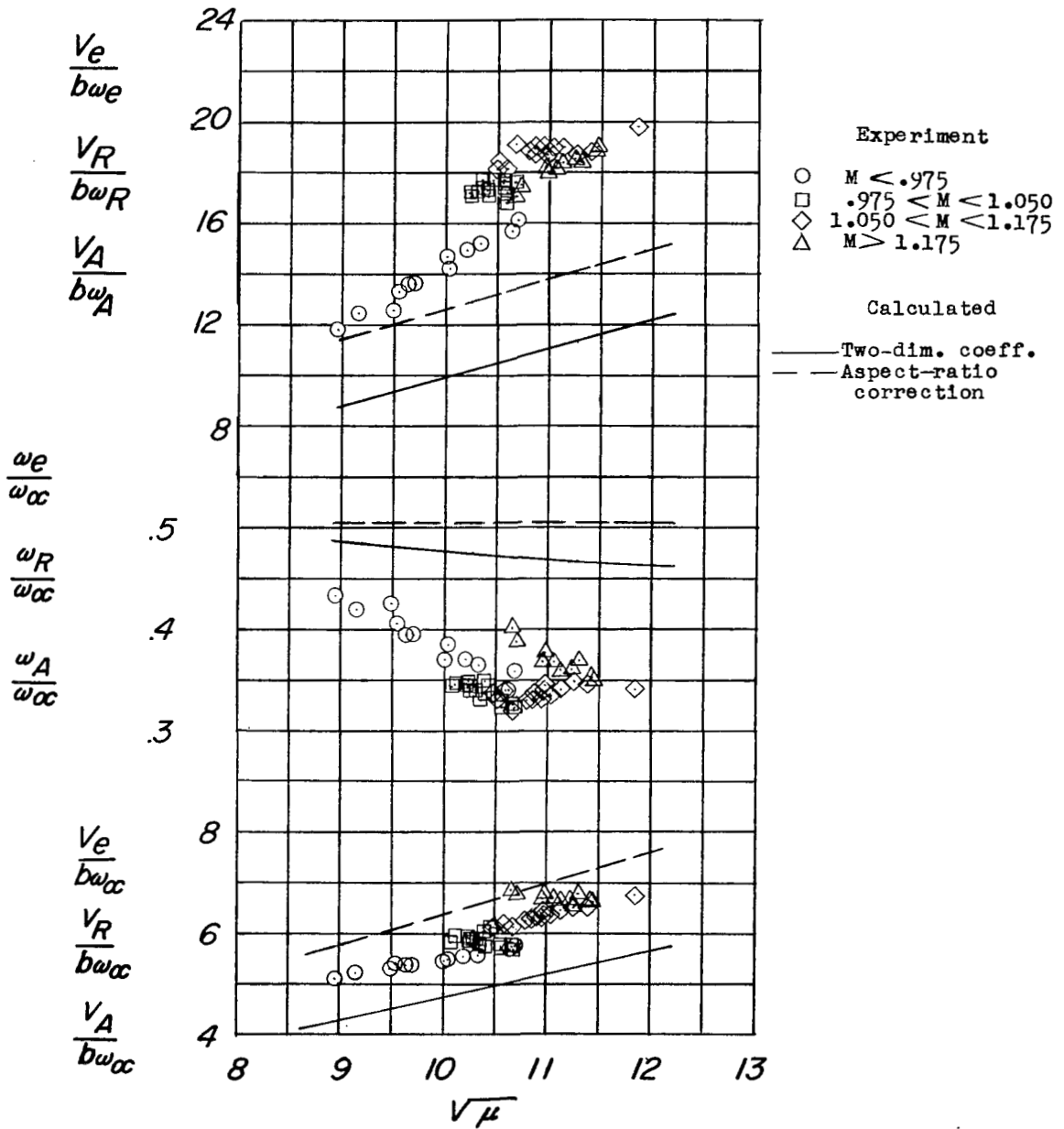


Figure 6.- Effect of mass ratio on the flutter characteristics.  $l/c = 1.61$ ; no fuselage.

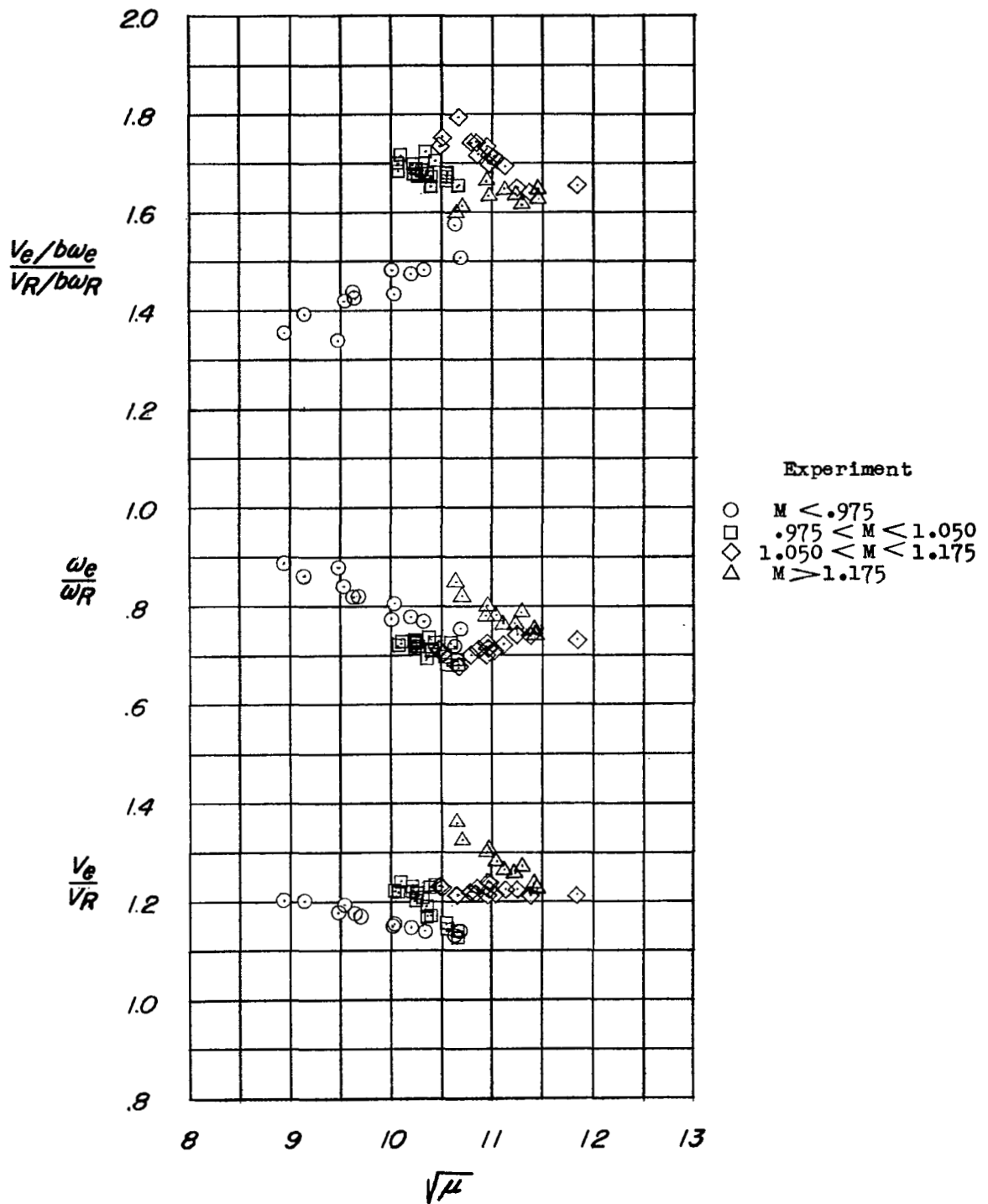


Figure 7.- Effect of mass ratio on normalized flutter characteristics.  
 $l/c = 1.61$ ; no fuselage.

~~CONFIDENTIAL~~

NASA Technical Library



3 1176 01437 2024

~~CONFIDENTIAL~~